Parameter and State Estimation in Vehicle Roll Dynamics

Rajesh Rajamani, Damrongrit Piyabongkarn, Vasilis Tsourapas, and Jae Y. Lew

***Abstract*—In active rollover prevention systems, a real-time rollover index, which indicates the likelihood of the vehicle to roll over, is used. This paper focuses on state and parameter estimation for reliable computation of the rollover index. Two key variables that are difficult to measure and play a critical role in the rollover index are found to be the roll angle and the height of the center of gravity of the vehicle. Algorithms are developed for real-time estimation of these variables. The algorithms investigated include a sensor fusion algorithm and a nonlinear dynamic observer. The sensor fusion algorithm requires a low-frequency tilt-angle sensor, whereas the dynamic observer utilizes only a lateral accelerometer and a gyroscope. The stability of the nonlinear observer is shown using Lyapunov's indirect method. The performance of the developed algorithms is investigated using simulations and experimental tests. Experimental data confirm that the developed algorithms perform reliably in a number of different maneuvers that include constant steering, ramp steering, double lane change, and sine with dwell steering tests.**

***Index Terms*—Cg height estimation, parameter estimation, roll angle estimation, roll dynamics, vehicle dynamics.**

I. Introduction

VEHICLE rollover accounts for a significant percentage of highway traffic fatalities. While only 3% of vehicle accidents result in rollovers, 33% of all fatalities have vehicle rollover as a contributing factor [1]. Hence, there is significant research being conducted on the development of active rollover prevention systems [2]–[14]. An active rollover prevention system typically utilizes differential braking to reduce the yaw rate of the vehicle and to slow down the vehicle speed. Both of these factors contribute to reducing the propensity of the vehicle to roll over.

An important challenge in the design of an active rollover prevention system is the calculation of the rollover index, which indicates the likelihood of the vehicle to roll over and is used to trigger differential braking to prevent rollover. Accurate calculation of the rollover index is important to ensure that rollovers can be prevented in time while, at the same, ensuring that active rollover prevention is not unnecessarily triggered.

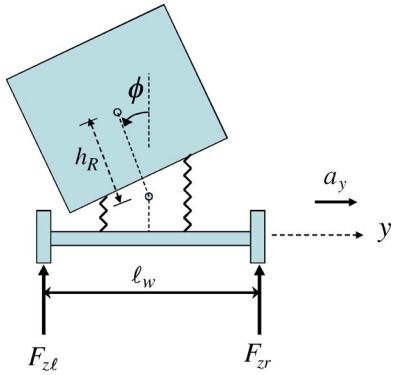

Fig. 1. Rollover index using lateral load transfer.

One method of defining the rollover index is based on the use of the real-time difference in vertical tire loads between the left and right sides of the vehicle. Fig. 1 shows a schematic of a vehicle with a sprung mass that undergoes roll motion. The difference between the vertical tire forces $F_{z\ell}$ and F_{zr} caused by the roll motion of the vehicle is used to define rollover index R as [9]

$$R = \frac{F_{z\ell} - F_{zr}}{F_{z\ell} + F_{zr}}. \tag{1}$$

If we assume that the roll motion of the sprung mass is entirely caused by the lateral acceleration of the vehicle (ignoring road and other external inputs) and assume that the unsprung mass of the vehicle is negligible, then it can be shown that the rollover index of (1) can be represented as [9]

$$R = \frac{2h_R a_y \cos\phi + 2h_R g \sin\phi}{\ell_w g} \tag{2}$$

where a_y is the lateral acceleration of the vehicle measured on the unsprung mass, ϕ is the roll angle, and h_R is the height of the center of gravity (c.g.) of the vehicle from the roll center of the sprung mass.

It should be noted that the rollover index of (2) needs the following:

1) measurement of lateral acceleration a_y;
2) roll angle ϕ;
3) knowledge of the track width ℓ_w;
4) knowledge of the height of the c.g. h_R.

Lateral acceleration is also required for the electronic stability control system [15], [16] on the vehicle and is typically available as a sensor measurement. However, roll angle cannot

Manuscript received March 7, 2011; revised June 3, 2011; accepted July 11, 2011. Date of publication September 8, 2011; date of current version December 5, 2011. The Associate Editor for this paper was L. Li.

R. Rajamani is with the University of Minnesota, Minneapolis, MN 55455 USA (e-mail: rajamani@me.umn.edu).

D. Piyabongkarn, V. Tsourapas, and J. Y. Lew are with the Innovation Center, Eaton Corporation, Eden Prairie, MN 55344 USA (e-mail: NengPiyabongkarn@eaton.com; VasiliosTsourapas@eaton.com; JaeYLew@eaton.com).

Color versions of one or more of the figures in this paper are available online at http://ieeexplore.ieee.org.

Digital Object Identifier 10.1109/TITS.2011.2164246

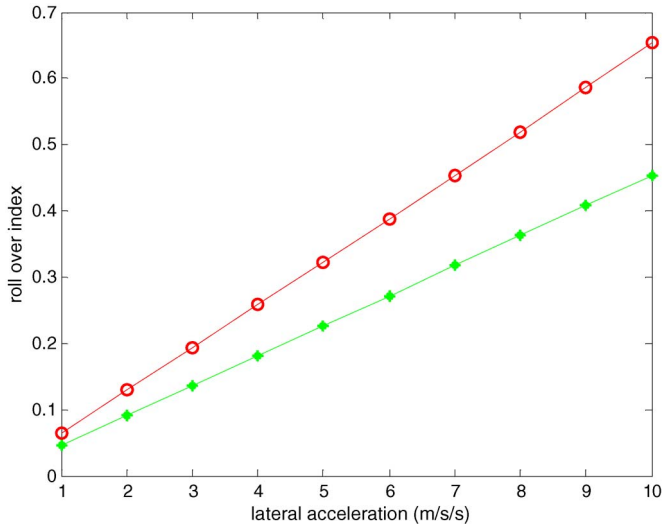

Fig. 2. Rollover indices (circle) R and (star) R_{approx} as a function of lateral acceleration.

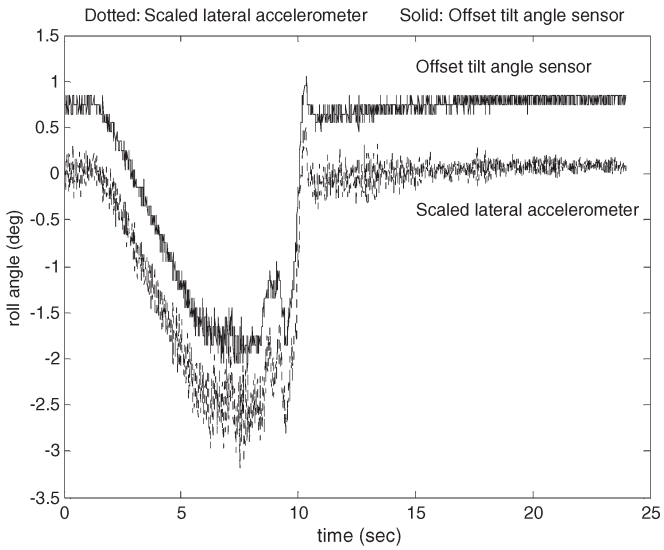

Fig. 3. Signals from tilt angle sensor and lateral accelerometer for swept steer experiment.

be easily measured in a vehicle. Suspension deflection measurements on the left and right sides of the vehicle are required to calculate roll angle. Since suspension deflection sensors are expensive, real-time measurement of the roll angle is typically not available on a passenger vehicle.

The track width ℓ_w is a parameter that remains constant and can be easily measured. The c.g. height h_R, on the other hand, cannot be directly measured. Sensors for real-time measurement of the c.g. height do not exist. While the c.g. height does *not* change in real time, it does change with the number of passengers and loading of the vehicle. In the case of sports utility vehicles (SUVs), military vehicles, and trucks, the c.g. height can significantly vary with cargo, with the variation being as much as 100% of the nominal height.

This paper therefore focuses on the accurate estimation of roll angle and the estimation of height of the c.g. of the vehicle to enable implementation of rollover index calculation of (2).

In literature and in commercial systems, the lack of roll angle measurement is typically handled by approximating the rollover index of (2) with

$$R_{\text{approx}} = \frac{2h_R a_y}{\ell_w g}. \tag{3}$$

Fig. 2 shows the original rollover index R and its approximation R_{approx} as a function of lateral acceleration during steady-state cornering around a circular track for a Volvo XC 90 SUV. It can be seen that the difference between the two curves increases as lateral acceleration increases, resulting in higher error during tight cornering maneuvers. Furthermore, the error increases with increase in the height of the c.g. Thus, the use of roll angle is important in an accurate calculation of the rollover index. This motivates the need to estimate roll angle.

A previous result on the estimation of the c.g. height has been provided by Solmaz *et al.* [17]. In [17], the c.g. height is estimated, assuming measurement of the full state is available. Alternately, transient effects are ignored, and a steady-state relationship between roll angle and lateral acceleration is used to determine the c.g. height at each sampling time instant. This paper develops a c.g. height estimation algorithm based on a more accurate roll dynamics model that includes transients and using a recursive least-squares (RLS) approach with a variable forgetting factor. Furthermore, the only sensors required are a roll rate gyroscope and a tilt angle sensor (which are the same as the sensors required for estimation of roll angle).

II. Kinematic Sensor Fusion

The following different systems can be considered for obtaining roll angle estimates on a vehicle:

1) use of a commercially available tilt angle sensor;
2) kinematic sensor fusion using both a tilt angle sensor and a gyroscope;
3) dynamic estimation of roll angle using a model-based observer.

The advantages and limitations of each of these systems are explored and illustrated in the succeeding paragraphs.

As a first step, consider a tilt angle sensor such as the Crossbow CXTD02 inertial angle sensor. The Crossbow tilt angle sensor consists of two two-axis in-built accelerometers and signal-processing algorithms that enable static tilt angle to be calculated from the accelerometer measurements. An example of an algorithm that can be used for this purpose can be found in [15].

A large SUV (military vehicle) was used for the experimental data described in the succeeding figures. Fig. 3 shows the signal from the tilt angle sensor for experiments conducted using the large SUV. In this experiment, a swept steer angle was used with the vehicle operating at a longitudinal speed of 50 mi/h. It can be seen that the tilt angle sensor closely tracks the lateral accelerometer signal after appropriate scaling. This is due to the fact that the angle calculation in the tilt sensor is based on the use of a lateral and a vertical accelerometer. Only the very low frequency portion of the tilt angle sensor signal is expected to be reliable. At high frequencies, changes in tilt angle are accompanied by significant accelerations due

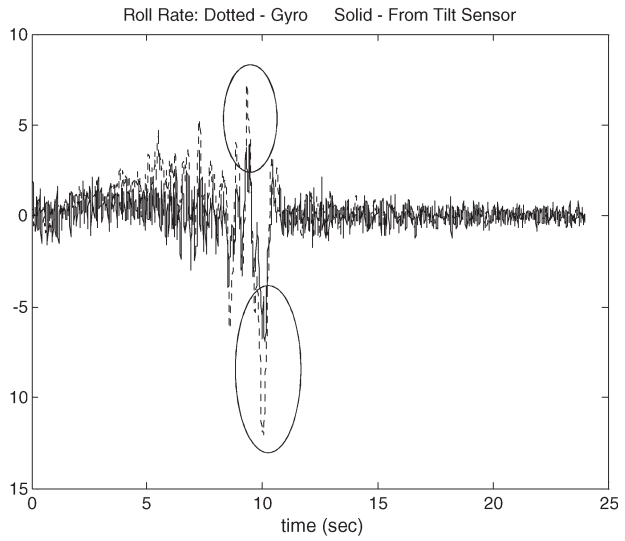

Fig. 4. Signals from gyroscope and differentiation of tilt angle sensor for swept steer.

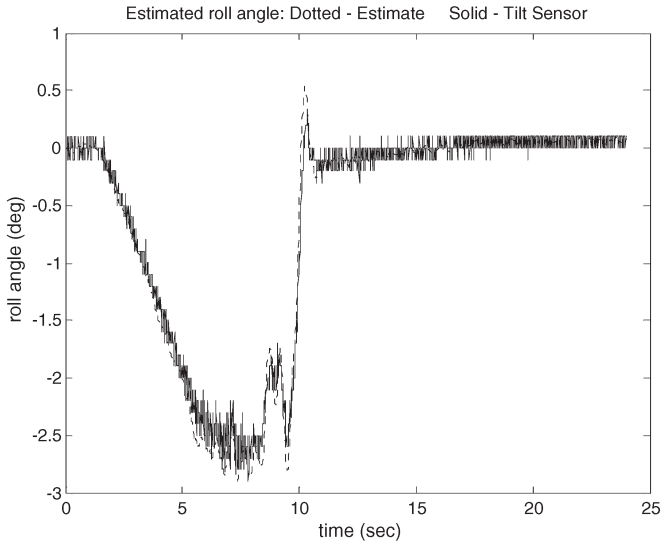

Fig. 5. Roll angle estimate from kinematic observer and tilt angle sensor.

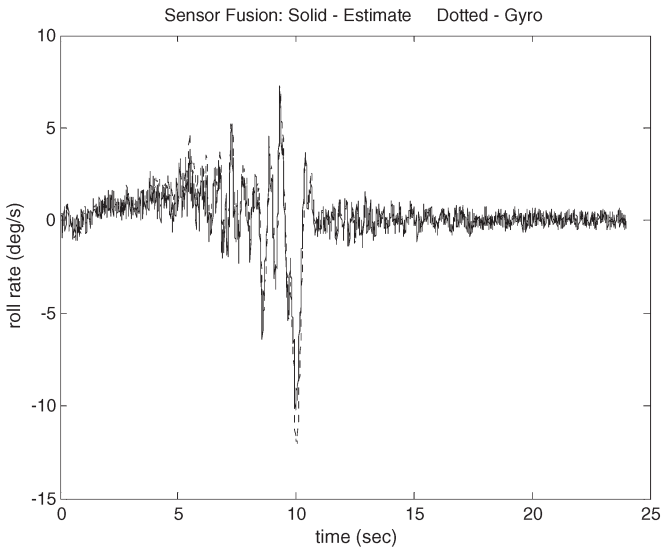

Fig. 6. Roll rate estimate from kinematic observer and gyroscope.

to which significant errors occur in the calculation of tilt angle from accelerometers.

The tilt angle sensor cannot provide a good measure of transient roll angle changes. This can be inferred by comparing the roll rate derived from the tilt sensor with the roll rate from a gyroscope. Fig. 4 shows a comparison of the roll rate, as measured by the gyroscope and as estimated from differentiation of the tilt angle sensor. It can be seen that the roll rate from differentiation of the tilt sensor lacks many of the transient features of the roll rate from the gyroscope. There is significant transient error in the tilt angle sensor, as shown by the circled portions of the curves in Fig. 4.

While the gyroscope can measure roll rate, the presence of a time-varying bias makes direct estimation of roll angle by integration of the gyroscope signal impossible.

Consider the use of both the gyroscope and the tilt angle sensor together to estimate the roll angle of the vehicle. Since the gyroscope can measure roll rate while the tilt angle sensor can measure static (or low-frequency) roll angle, the signals from the two sensors can be combined to obtain good estimates of both roll angle and roll rate. The following kinematic fusion algorithm is suggested:

$$\dot{\hat{\phi}} = \dot{\phi}_{\text{gyro}} + k(\phi_{\text{tilt sensor}} - \hat{\phi}). \tag{4}$$

In the frequency domain, the relation between the estimated roll angle $\hat{\phi}$ and the gyroscope roll rate and tilt-angle-sensor-measured roll angle is given as follows:

$$\hat{\phi} = \frac{1}{s+k}\dot{\phi}_{\text{gyro}} + \frac{k}{s+k}\phi_{\text{tilt sensor}}. \tag{5}$$

Thus, the estimate combines the low-frequency content of the angle estimate from the tilt sensor with the high-frequency content of the integrated signal from the gyroscope. This helps eliminate the drift from integration of the gyroscope. Note that the algorithm is stable for all values of k.

Fig. 5 shows the roll angle estimate as estimated by the kinematic algorithm of (4). It can be seen that the estimated roll angle tracks the steady-state tilt angle signal, except for better transient performance it provides during the period between 9 and 11 s. Fig. 6 shows the roll rate as estimated by the kinematic algorithm and by the gyroscope. It can be seen that the roll rate estimate from the kinematic algorithm is a far better match for the gyroscope signal than the roll rate as estimated from differentiation of the tilt angle sensor, as previously studied in Fig. 4.

III. Dynamic Observer

An alternate approach to estimation of roll angle is to use an observer based on a dynamic model of the vehicle roll dynamics, using only lateral acceleration and a roll rate gyroscope as the measurements for the observer. Since a lateral accelerometer is required by default for rollover index calculation, the only additional sensor being used here then is the roll rate gyroscope.

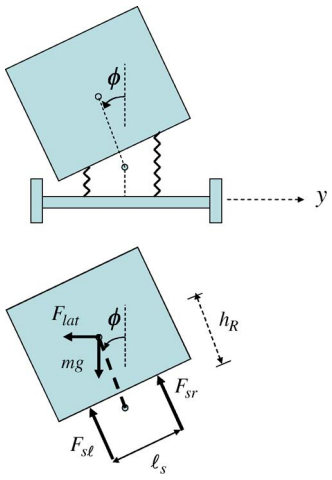

Fig. 7. Roll dynamics and free-body diagram.

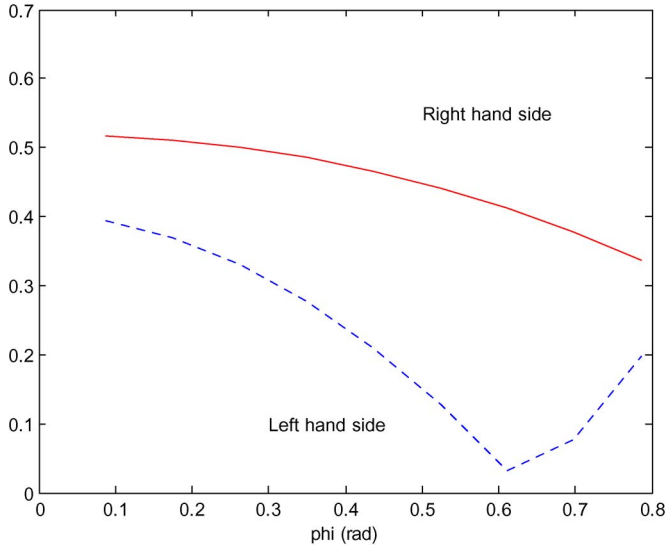

Fig. 8. Suspension forces.

The need for the tilt angle sensor is eliminated. It should be noted that the current retail cost of a tilt angle sensor is on the order of $100.

Estimation of roll angle using only an accelerometer has been previously presented in [5]. However, the results in [5] assume a steady-state algebraic relation between lateral acceleration and roll angle, ignoring transient dynamics. Furthermore, a gravitational term and several trigonometric terms are also ignored in [5].

To develop a dynamic model for the roll dynamics of the vehicle, consider the free-body diagram in Fig. 7.

It should be noted that d'Alembert's force $F_{\rm lat}$ is applied at the c.g. of the vehicle. It is also assumed that the suspension forces on the sprung mass act parallel to the sprung mass z-axis. Vertical force balance yields the sum of the suspension forces as

$$F_{sl} + F_{sr} = mg. \tag{6}$$

Taking moments about the roll center, the roll dynamics equation can be written as

$$\begin{aligned}\left(I_{xx} + mh_R^2\right)\ddot{\phi} &= \sum M_x \\ &= F_{\rm lat} h_R \cos\phi + mgh_R \sin\phi \\ &\quad - F_{sl}\frac{\ell_s}{2} + F_{sr}\frac{\ell_s}{2}\end{aligned} \tag{7}$$

or

$$\left(I_{xx}+mh_R^2\right)\ddot{\phi} = F_{\rm lat} h_R \cos\phi + mgh_R \sin\phi + \frac{\ell_s}{2}(F_{sr}-F_{sl}). \tag{8}$$

Suspension forces F_{sl} and F_{sr} act on both sides of the suspension springs (Fig. 8). The suspension deflections on the left and right sides due to roll are given as follows:

$$z_{s\ell} = -\frac{\ell_s}{2}\sin\phi \tag{9}$$

$$z_{sr} = \frac{\ell_s}{2}\sin\phi. \tag{10}$$

Hence, the suspension forces are

$$F_{sl} = \frac{mg}{2} + k\frac{\ell_s}{2}\sin(\phi) \tag{11}$$

$$F_{sr} = \frac{mg}{2} - k\frac{\ell_s}{2}\sin(\phi) \tag{12}$$

$$F_{sl} - F_{sr} = k\ell_s \sin\phi. \tag{13}$$

Substituting (13) into (8) yields

$$\left(I_{xx} + mh_R^2\right)\ddot{\phi} = F_{\rm lat} h_R \cos\phi + mgh_R \sin\phi - \frac{1}{2}k\ell_s^2 \sin\phi. \tag{14}$$

Including suspension damping in addition to stiffness, the roll dynamics model can finally be written down as

$$\begin{aligned}\left(I_{xx} + mh_R^2\right)\ddot{\phi} &= ma_y h_R \cos\phi + mgh_R \sin\phi \\ &\quad -\frac{1}{2}k\ell_s^2 \sin\phi - \frac{1}{2}c\ell_s^2(\cos\phi)\dot{\phi}.\end{aligned} \tag{15}$$

It should be noted that the roll dynamics depend on the lateral dynamics through the lateral acceleration term a_y. By avoiding further expansion of this term in terms of lateral tire forces and lateral dynamic states, a complicated coupled set of equations between roll and lateral dynamics is avoided. Instead, the variable a_y is assumed to be measured.

The following observer is proposed to estimate roll angle:

$$\dot{\hat{\phi}} = \dot{\phi}_{\rm meas} + k(\hat{\phi}_{\ell f} - \hat{\phi}) \tag{16}$$

$$\begin{aligned}\left(I_{xx} + mh_R^2\right)\ddot{\hat{\phi}}_{\ell f} &= ma_y h_R \cos\phi_{\ell f} + mgh_R \sin\phi_{\ell f} \\ &\quad - \frac{k}{2}\ell_s^2 \sin\phi_{\ell f} - \frac{c}{2}\ell_s^2(\cos\phi_{\ell f})\dot{\phi}_{\ell f}.\end{aligned} \tag{17}$$

The first equation in the observer (16) combines the integrated roll rate from the gyroscope with a low-frequency roll angle estimate provided by the (17). Equation (17) is a replica

of the roll-dynamics-model-based equation. Hence, the steady-state roll angle estimate from (17) should converge to the actual steady-state roll angle of the stable dynamics of (15). As the analysis here shows, the steady-state roll angle converges to zero in the absence of lateral acceleration and to the steady-state value given by (18), shown below, in the presence of lateral acceleration.

Analysis of Observer Stability: With the equation of motion given by (15) and with the condition $(1/2)k\ell_s^2 > mgh_R$ being satisfied, the steady-state roll angle converges to zero in the absence of lateral acceleration for all roll angles satisfying $|\phi| \leq \phi_m$, where ϕ_m depends on the parameters of the roll dynamics equation and is typically greater than 30°. In the presence of lateral acceleration, the steady-state roll angle converges to

$$\phi_{ss} = \frac{a_y}{\frac{k\ell_s^2}{2mh_R} - g} \tag{18}$$

for all roll angles satisfying $|\phi| \leq \phi_m$.

Proof: The equation of motion (15) can be rewritten in short notation in the absence of lateral acceleration as

$$\ddot{\phi} = -a\sin\phi - b\dot{\phi}\cos\phi \tag{19}$$

where a and b are positive constants. Let a Lyapunov function candidate be given by

$$V = [\phi \quad \dot{\phi}]^T P[\phi \quad \dot{\phi}] = p_1\phi^2 + p_2\dot{\phi}^2 + 2p_3\phi\dot{\phi}. \tag{20}$$

To ensure that V is positive definite, the following constraint between p_1, p_2, and p_3 needs to be satisfied:

$$\sqrt{p_1p_2} > p_3. \tag{21}$$

Note that, if (21) is satisfied, then p_3 can be rewritten as

$$p_3 = (\sqrt{\alpha p_1})(\sqrt{\beta p_2}) \tag{22}$$

with $\alpha < 1$ and $\beta < 1$.

Then

$$\begin{aligned} V &= p_1\phi^2 + p_2\dot{\phi}^2 + 2p_3\phi\dot{\phi} \\ &= (1-\alpha)p_1\phi^2 + (1-\beta)p_2\dot{\phi}^2 + \alpha p_1\phi^2 \\ &\quad + \beta p_2\dot{\phi}^2 + 2(\sqrt{\alpha p_1})(\sqrt{\beta p_2})\phi\dot{\phi} \end{aligned}$$

or

$$V = (1-\alpha)p_1\phi^2 + (1-\beta)p_2\dot{\phi}^2 + (\phi\sqrt{\alpha p_1} + \dot{\phi}\sqrt{\beta p_2})^2$$

which is positive definite.

Taking derivatives of the Lyapunov function candidate

$$\begin{aligned} \dot{V} &= 2p_1\phi\dot{\phi} + 2p_2\dot{\phi}\ddot{\phi} + 2p_3\phi\ddot{\phi} + 2p_3\dot{\phi}^2 \\ \dot{V} &= 2p_1\phi\dot{\phi} - 2p_2\dot{\phi}a\sin\phi - 2p_3a\phi\sin\phi \\ &\quad - 2p_2\dot{\phi}^2\cos\phi - 2p_3b\phi\dot{\phi}\cos\phi + 2p_3\dot{\phi}^2 \end{aligned}$$

or

$$\begin{aligned} \dot{V} = \phi\dot{\phi}[2p_1 - 2bp_3\cos\phi] - 2p_2\dot{\phi}a\sin\phi \\ + \dot{\phi}^2[-2p_2\cos\phi + 2p_3] - 2p_3a\phi\sin\phi. \end{aligned} \tag{23}$$

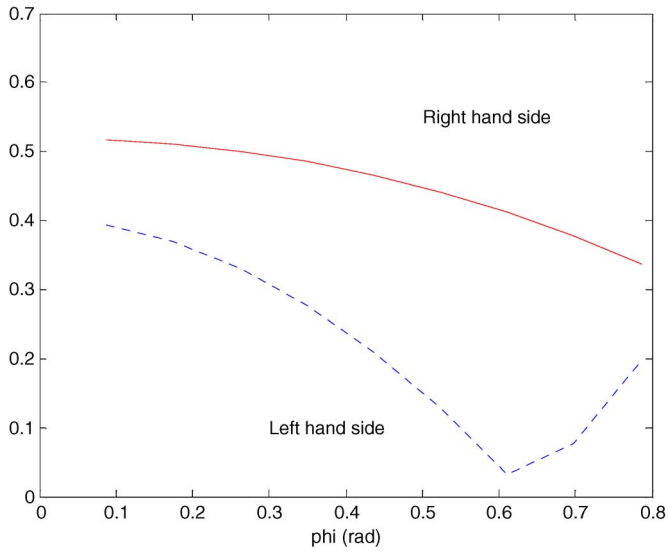

Fig. 9. Right- and left-hand sides of (24).

The last two terms are negative definite, as long as $p_3 > p_2\cos\phi$.

We need to ensure that the term $\phi\dot{\phi}[2p_1 - 2bp_3\cos\phi - 2p_2a(\sin\phi/\phi)]$ is dominated by the last two terms so that $\dot{V}$ is negative definite. This can be done by choosing p_1, p_2, and p_3 such that

$$\begin{aligned} \left[2p_1 - 2bp_3\cos\phi - 2p_2a\frac{\sin\phi}{\phi}\right] \\ \leq (\sqrt{2p_2\cos\phi - 2p_3})\left(\sqrt{2ap_3\frac{\sin\phi}{\phi}}\right). \end{aligned} \tag{24}$$

The left- and right-hand sides of (24) are plotted in Fig. 9 for roll angles ranging from 0 to 0.8 rad (see Table I for vehicle parameters). It can be seen that inequality (24) is satisfied for all of these roll angles, thus showing that the Lyapunov function derivative is negative; hence, the steady-state roll angle will converge to zero.

In the case when lateral acceleration is nonzero, the steady-state roll angle can be obtained by setting $\dot{\phi} = \ddot{\phi} = 0$ in (15) to obtain the steady-state value in (18).

Since (15) and (17) have identical dynamics, the steady-state roll angle of the estimator in (17) will be identical to that of the original system. Hence, the low-frequency dynamics of the observer in (16) are determined by the estimate from (17), whereas the high-frequency dynamics are obtained from integration of the gyroscope.

It should be noted that use of the observer in (16) and (17) requires knowledge of the roll inertia, height of the c.g., and suspension spring stiffness. Knowledge of the damping coefficient is not important since it only affects the transient performance of the observer and not the steady-state value. The transient performance can be obtained from fusion with the gyroscope signal, as in (16).

IV. Experimental Results With Dynamic Observer

Fig. 10 shows the tilt angle sensor signal for steering, consisting of a sine with dwell maneuver. Again, it can be seen that the

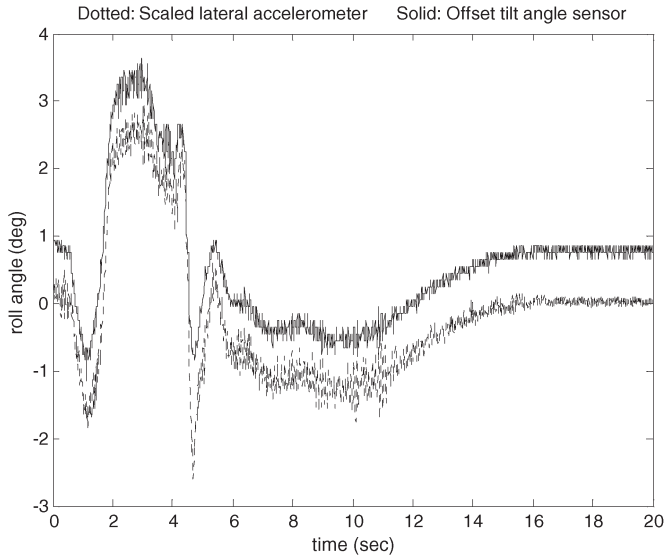

Fig. 10. Tilt angle sensor and accelerometer signals for FMVSS data.

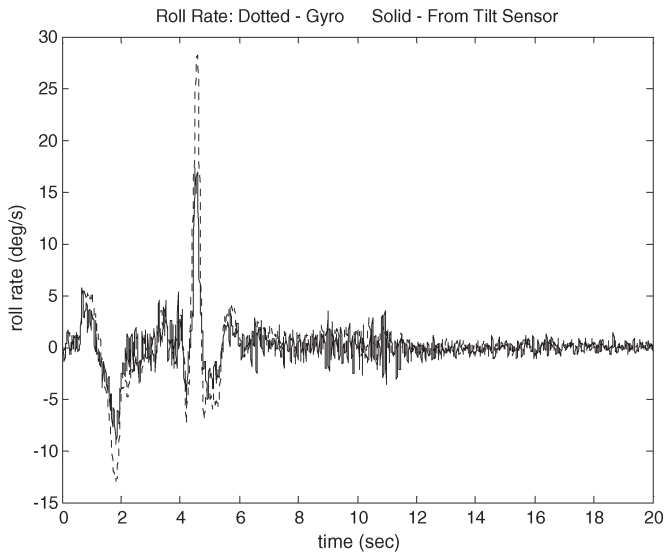

Fig. 11. Roll rate from gyroscope and differentiation of tilt angle signal for FMVSS data.

tilt angle sensor signal closely tracks the lateral accelerometer signal. However, as shown in Fig. 11, the differentiated tilt sensor signal has significant transient error, compared with the roll rate signal, as measured by the gyroscope.

Fig. 12 shows the estimated roll angle using the dynamic observer of (14) and (15). It can be seen that the roll angle tracks the steady-state values of the tilt angle sensor but has significantly richer transient features in its signal, which is seen particularly in the time duration between 4 and 7 s in the shown plot.

Fig. 13 shows the estimated roll rate from the dynamic observer. It can be seen that the estimated roll rate matches the roll rate signal from the gyroscope much better than the differentiated tilt angle signal.

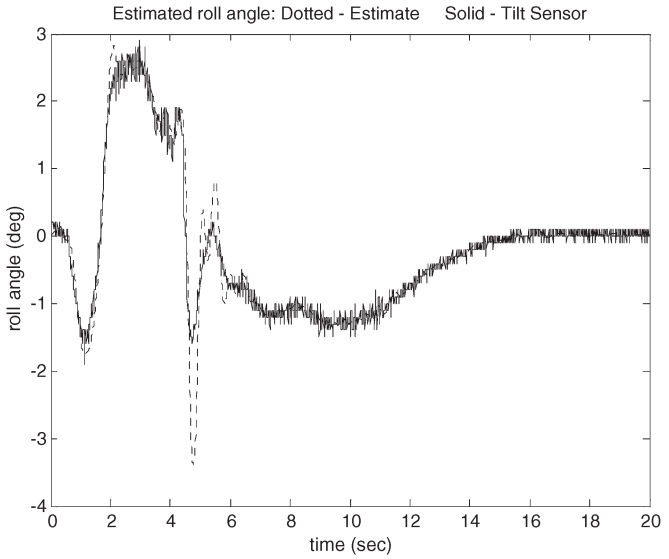

Fig. 12. Roll angle estimated from dynamic observer.

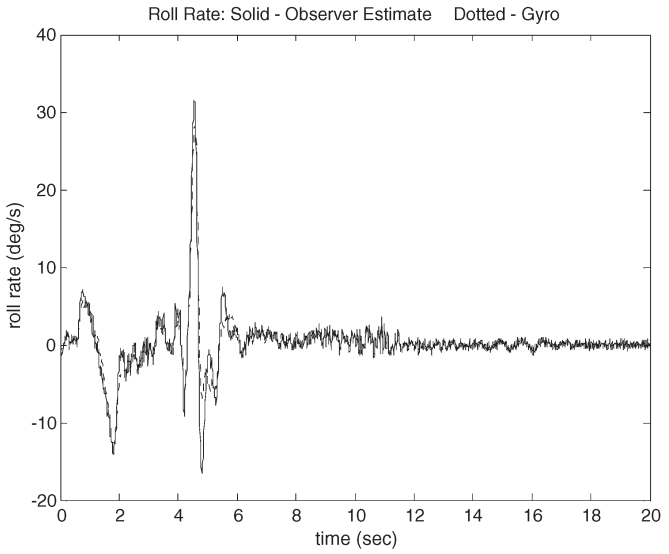

Fig. 13. Roll rate estimated from dynamic observer.

V. Center of Gravity Height Estimation

As described in Section I, the height of the c.g. of the vehicle plays an important role in the computation of the rollover index. The c.g. height can significantly change in SUVs, military vehicles (due to top loading), and trucks. Furthermore, there is no convenient method available to measure c.g. height. Unlike longitudinal c.g. position, which can be obtained by measuring weights at the front axle and rear axle at a weigh station, there is no convenient technique for measuring c.g. height.

This section proposes and experimentally evaluates an algorithm for c.g. height estimation.

Formulation 1: Start with the following model for the roll dynamics of the vehicle:

$$\left(I_{xx} + mh_R^2\right)\ddot{\phi} = ma_y h_R \cos\phi + mgh_R \sin\phi - \frac{1}{2}k\ell_s^2 \sin\phi - \frac{1}{2}c\ell_s^2(\cos\phi)\dot{\phi}. \quad (25)$$

At steady-state conditions (during steady cornering), the roll rate and acceleration can be assumed to be constant. In that case, (25) becomes

$$0 = ma_y h_R \cos\phi + mgh_R \sin\phi - \frac{1}{2}k\ell_s^2 \sin\phi \tag{26}$$

or

$$h_R(ma_y \cos\phi + mg\sin\phi) = \frac{1}{2}k\ell_s^2 \sin\phi. \tag{27}$$

This can be rewritten in a parameter identification form as

$$y = \psi^T \theta \tag{28}$$

with

$$y = \frac{k}{2}\ell_s^2 \sin\phi$$

$$\psi = ma_y \cos\phi + mg\sin\phi, \text{ and } \theta = h_R. \tag{29}$$

Formulation 2: Alternatively, without assuming steady-state cornering, the transient dynamics of (25) can be accounted for by using

$$y = \frac{k}{2}\ell_s^2 \sin\phi + \frac{c}{2}\ell_s^2 \dot{\phi}\cos\phi + I_{xx}\frac{s}{\tau s + 1}\dot{\phi}$$

$$\psi = ma_y \cos\phi + mg\sin\phi \tag{30}$$

where s is the Laplace operator, and the influence of the term mh_R^2 has been ignored and assumed to be significantly smaller than I_{xx}.

RLS Identification: Define error $e(t)$ as

$$e(t) = y(t) - \psi(t)^T \hat{\theta}(t) \tag{31}$$

where $\hat{\theta}(t)$ is the vector of estimated parameters, $\psi(t)$ is the regression vector, and $y(t)$ is the measured output.

The RLS algorithm [18] will be used in this paper to iteratively update the unknown parameter vector $\hat{\theta}(t)$, at each sampling time, using the past input and output data contained within the regression vector $\psi(t)$. The RLS algorithm updates the unknown parameters to minimize the sum of the squares of the modeling errors. The procedure of the RLS algorithm at each time step $t = k\Delta T$, with ΔT being the sampling time, is given as follows:

Step 1) Measure the system output $y(k)$, and calculate the regression vector $\psi(k)$.

Step 2) Calculate the identification error $e(k)$, which is the difference between the system's actual output at this time and the predicted model output obtained from the estimated parameters in the previous sample, $\hat{\theta}(k-1)$, i.e.,

$$e(k) = y(k) - \psi(k)^T \hat{\theta}(k-1). \tag{32}$$

Step 3) Calculate the updated gain vector $K(k)$ as

$$K(k) = \frac{P(k-1)\psi(k)}{\lambda + \psi^T(k)P(k-1)\psi(k)} \tag{33}$$

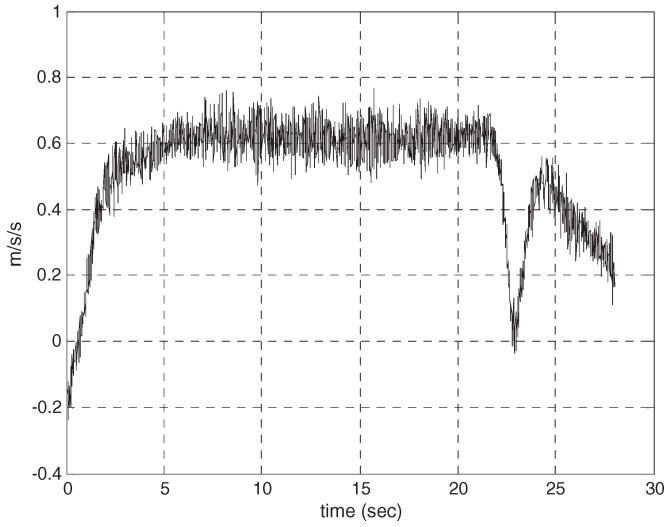

Fig. 14. Lateral acceleration in constant steering maneuver.

and calculate the covariance matrix $P(k)$ using

$$P(k) = \frac{1}{\lambda}\left[P(k-1) - \frac{P(k-1)\psi(k)\psi^T(k)P(k-1)}{\lambda + \psi^T(k)P(k-1)\psi(k)}\right]. \tag{34}$$

Step 4) Update the parameter estimate vector $\theta(k)$ as

$$\theta(k) = \theta(k-1) + K(k)e(k). \tag{35}$$

The parameter λ is called the forgetting factor. It is used to effectively reduce the influence of old data that may no longer be relevant to the model. This allows the parameter estimates to quickly track changes in the process. A typical value for λ is in the interval (0.9, 1).

While (32)–(35) can be used to estimate the height of the c.g. in real time, an important issue needs to be noted:

This algorithm requires that the roll angle be nonzero. In the case where the roll angle is zero, as when the car is being driven straight with zero steering, both the left- and right-hand sides of (27) are zero.

Hence, to apply this technique for c.g. height estimation, it is required that the data used be from a maneuver in which the vehicle is under a cornering maneuver with nonzero steering. Since c.g. height is a quasi-constant parameter and does not change for long periods of time, it is a viable approach to wait for a cornering maneuver to do the c.g. height estimation. In the case of the experimental results described here, the algorithm was set to update the parameter estimates only when the lateral acceleration of the vehicle exceeded a threshold of 0.5 m/s^2.

Fig. 14 shows lateral acceleration for a constant steering angle maneuver on the same experimental vehicle, as described earlier. As seen in the figure, lateral acceleration is approximately constant between 6 and 21 s in the data.

The estimated c.g. height using the algorithm with formulation 1 of (27) is shown in Fig. 15. In this case, a forgetting factor of $\lambda = 0.995$ was used. With this large forgetting factor, almost all of the data is used in the recursive calculations, leading to a smooth noise-free estimate, with a steady-state value of about

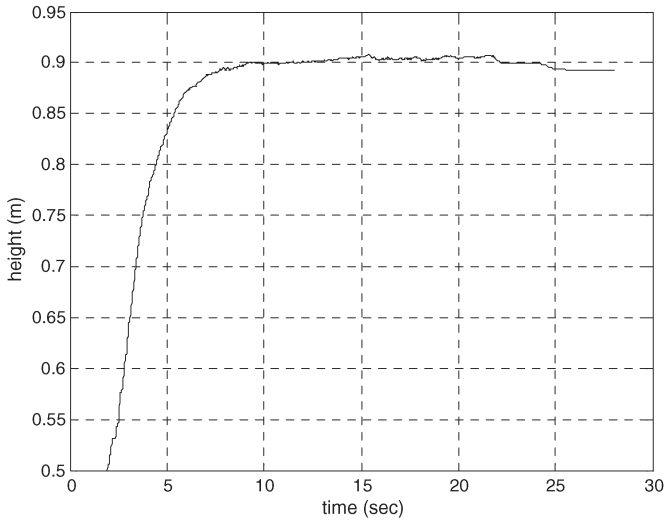

Fig. 15. Estimated c.g. height using a forgetting factor of 0.995.

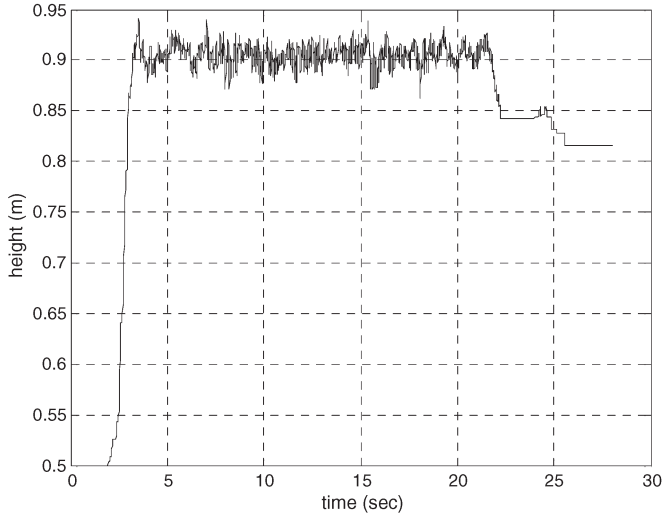

Fig. 16. Estimated c.g. height using a forgetting factor of 0.9.

0.9 m. However, it takes almost 5 s for the estimated c.g. height value to converge to 90% of its steady-state value.

Faster convergence can be obtained using a smaller forgetting factor. A forgetting factor of $\lambda = 0.9$ was used in Fig. 16. It can be seen that the estimate now quickly converges within a second. However, it has significant noise at steady state. To achieve a noise-free steady-state estimate while also obtaining quick convergence, a variable forgetting factor was used in the data shown in Fig. 17.

For the variable forgetting factor, the identification error $e(k)$ is monitored throughout the period of contact. An alarm is signaled if the identification error has been larger than a threshold for a certain amount of time. The recursive formula of this method is shown as

$$a_k = \max\left(a_{k-1} + |e_k| - d, 0\right), \quad k = 1, 2, \ldots$$
$$a_0 = 0.$$

As can be seen, given the identification error e_k calculated in an ordinary RLS as the input, an output alarm signal can be generated. If the alarm value $a_k > h$, a smaller forgetting

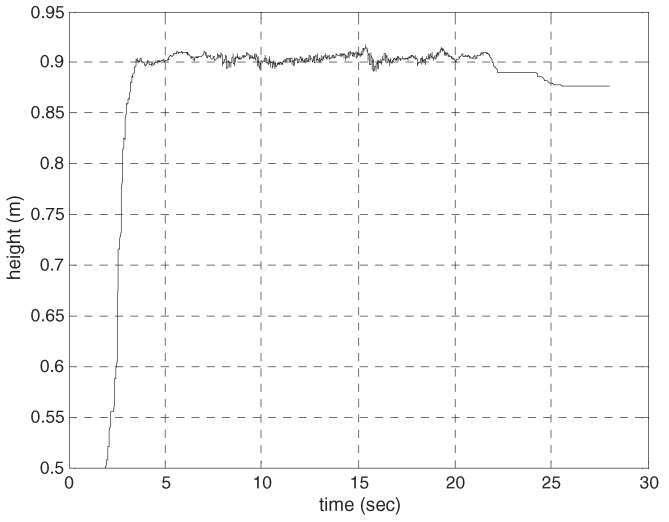

Fig. 17. Estimated c.g. height using a variable forgetting factor.

factor will be chosen in the RLS. Here, the threshold value h is used to determine when the forgetting factor should be adjusted, in the condition that an alarm signal has been on for a sufficiently long time. The other threshold value d in the preceding equation is used to judge when to turn on the alarm. This makes the process ignore errors smaller than d. If the estimation system can swiftly track any abrupt change in parameter, the identification error will drop below the threshold, thus resulting in a zero value of the alarm signal. At this stage, the alarm is turned back off, and a larger forgetting factor is chosen for its high immunity to noise at steady state.

Fig. 18 shows lateral acceleration for a swept steering maneuver in which the steering angel continuously increases and then briefly remains a constant. The corresponding c.g. height estimate from the algorithm is shown in Fig. 19. It can be seen in Fig. 19 that the estimate varies quite a bit in the range between 0.85 and 0.97 m. This variation happens due to the nonsteady nature of the steering maneuver since the roll rate and roll acceleration no longer satisfy the zero transient dynamics assumption of (27). However, it can be seen from the figure that an approximate estimate of c.g. height can still be obtained under these conditions.

Formulation 1 using (27) assumes steady-state cornering in which the roll angle is constant. Hence, it will lead to errors during time periods when the roll rate and roll acceleration are nonzero. Formulation 2 does not require roll rate and roll acceleration to be zero. It requires the measurement of roll rate and roll acceleration. Roll acceleration is obtained by numerical differentiation of roll rate in (30).

The estimated c.g. height using formulation 2 is shown in Fig. 20. It can be seen that the variation of the c.g. height estimate is less than the variation of the previous formulation in Fig. 19.

VI. Conclusion

The roll angle and height of the c.g. are important variables that play a critical role in the calculation of real-time rollover index for a vehicle. Sensors for measuring roll angle are

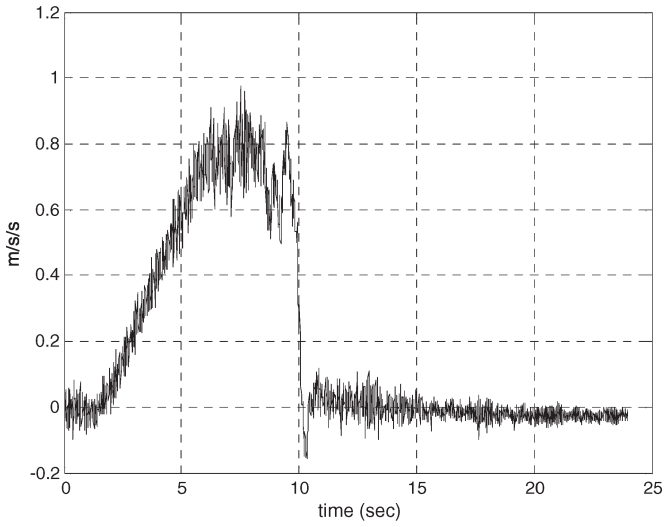

Fig. 18. Lateral acceleration during a swept steering maneuver.

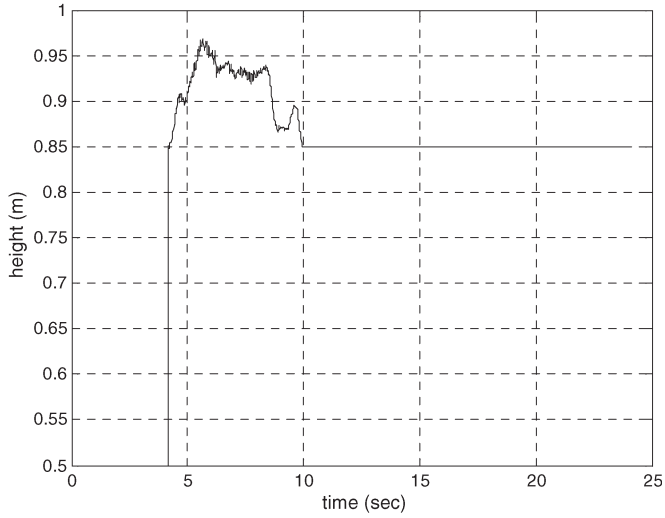

Fig. 19. Estimated c.g. height in swept steering maneuver.

expensive. Sensors for directly measuring the c.g. height of a vehicle in real time do not exist.

This paper has focused on algorithms to estimate real-time roll angle and c.g. height. The algorithms investigated include a sensor fusion algorithm that utilizes a low-frequency tilt angle sensor and a gyroscope, and a nonlinear dynamic observer that utilizes only a lateral accelerometer and a gyroscope. The first algorithm entails additional cost for the tilt angle sensor but is a simple, reliable, and robust algorithm. The second algorithm does not need the additional sensor but requires knowledge of the roll dynamics model. The performance of the developed algorithms has been investigated using experimental tests on a large SUV. Experimental data have confirmed that the developed algorithms reliably performed in a number of different maneuvers that include constant steering, ramp steering, and sine with dwell steering tests.

The c.g. height estimation algorithm performs well during maneuvers with changing steering angle if terms related to roll velocity and roll acceleration are included in the parameter identification equation.

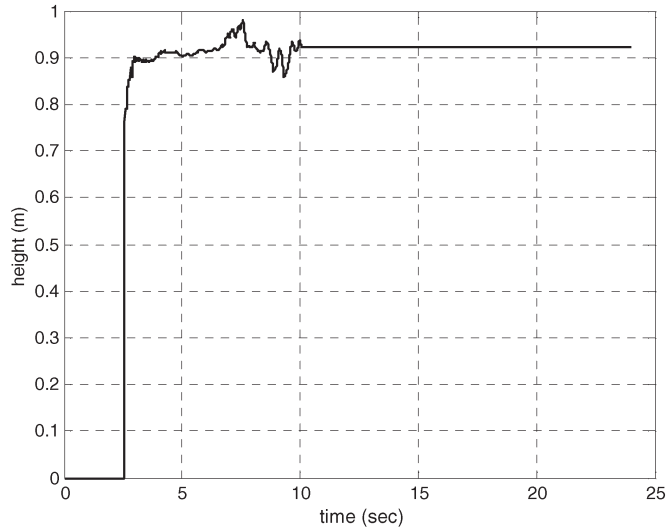

Fig. 20. Estimated c.g. height using formulation 2.

TABLE I
TABLE OF PARAMETER VALUES

Symbol	Description	Parameter value
m	Vehicle mass	2205 kg
I_{xx}	Vehicle roll moment of inertia about c.g.	5512.5 kg m^2
ℓ_w	Track width	1.75 m
h_R	Height of c.g. from roll center	0.7 m
k	Suspension stiffness	20000 N/m
c	Suspension damping	3900 Ns/m
ℓ_s	Distance between left and right suspensions	1.5 m

The results in this paper provide solutions that will enable accurate calculation of rollover index, thus enabling better rollover prevention systems to be developed.

REFERENCES

[1] Nat. Hwy. Traffic Safety Admin., U.S. Dept. Transp., Fatality Analysis Reporting System, 2003. [Online]. Available: http://www-fars.nhtsa.dot.gov/Main/index.aspx

[2] T. J. Wielenga and M. A. Chace, "A study in rollover prevention using anti-rollover braking," presented at the SAE World Congr., Detroit, MI, 2000, SAE Paper 2000-01-1642.

[3] C. R. Carlson and J. C. Gerdes, "Optimal rollover prevention with steer by wire and differential braking," in *Proc. ASME Int. Mech. Eng. Congr. Expo.*, Nov. 2003, pp. 345–355.

[4] G. J. Forkenbrock, W. R. Garrott, M. Heitz, and B. C. O'Harra, "Experimental examination of J-turn and Fishhook maneuver that may induce on-road untripped light vehicle rollover," presented at the SAE World Congr., Detroit, MI, 2003, SAE Paper 2003-01-1008.

[5] A. Hac, T. Brown, and J. Martens, "Detection of Vehicle Rollover," presented at the SAE World Congr., Detroit, MI, 2004, SAE Tech. Paper Series 2004-01-1757.

[6] J. Y. Lew, D. Piyabongkarn, and J. A. Grogg, "Minimizing dynamic rollover propensity with electronic limited slip differentials," SAE Book Number V115-6, *SAE Trans. J. Passenger Cars: Mech. Syst.*, pp. 1183–1190, 2006.

[7] E. K. Liebemann, K. Meder, J. Schuh, and G. Nenninger, "Safety and performance enhancement: The Bosch electronic stability control (ESP)," presented at the SAE World Congr., Detroit, MI, 2004, SAE Paper 2004-21-0060.

[8] P. J. Liu, S. Rakheja, and A. K. W. Ahmed, "Detection of dynamic roll instability of heavy vehicles for open-loop rollover control," presented at the Future Transportation Technology Conf. Expo., San Diego, CA, 1997, SAE Paper 973 263.

[9] D. Odenthal, T. Bunte, and J. Ackermann, "Nonlinear steering and braking control for vehicle rollover avoidance," in *Proc. Eur. Control Conf.*, 1999, pp. 1–6.
[10] S. Takano and M. Nagai, "Dynamic control of large vehicles for rollover prevention," in *Proc. IEEE IVEC*, 2001, pp. 85–89.
[11] H. E. Tseng, B. Ashrafi, D. Madau, T. A. Brown, and D. Recker, "The development of vehicle stability control at Ford," *IEEE/ASME Trans. Mechatron.*, vol. 4, no. 3, pp. 223–234, Sep. 1999.
[12] K. Yi, J. Yoon, and D. Kim, "Model-based estimation of vehicle roll state for detection of impending vehicle rollover," in *Proc. Amer. Control Conf.*, New York, Jul. 11–13, 2007, pp. 1624–1629.
[13] J. Yoon, D. Kim, and K. Yi, "Design of a rollover index based vehicle stability control scheme," *Vehicle Syst. Dyn.*, vol. 45, no. 5, pp. 459–475, May 2007.
[14] S. Solmaz, M. Corless, and R. Shorten, "A methodology for the design of robust rollover prevention controllers for automotive vehicles with active steering," *Int. J. Control*, vol. 80, no. 11, pp. 1763–1779, Nov. 2007.
[15] D. Piyabongkarn, R. Rajamani, J. Grogg, and J. Lew, "Development and experimental evaluation of a slip angle estimator for vehicle stability control," *IEEE Trans. Control Syst. Technol.*, vol. 17, no. 1, pp. 78–88, Jan. 2009.
[16] R. Rajamani, *Vehicle Dynamics and Control*. New York: Springer-Verlag, 2005, p. 471.
[17] S. Solmaz, M. Akar, R. Shorten, and J. Kalkkuhl, "Realtime multiple-model estimation of center of gravity position in automotive vehicles," *Veh. Syst. Dyn. J.*, vol. 46, no. 9, pp. 763–788, 2008.
[18] S. Sastry and M. Bodson, *Adaptive Control: Stability, Convergence and Robustness*. Englewood Cliffs, NJ: Prentice-Hall, 1989.

Rajesh Rajamani received the B.Tech. degree from Indian Institute of Technology Madras, Chennai, India, in 1989 and the M.S. and Ph.D. degrees from the University of California, Berkeley, in 1991 and 1993, respectively.

He is currently a Professor of mechanical engineering with the University of Minnesota, Minneapolis. He has authored more than 80 journal papers and is a co-inventor on seven patent applications. He is the author of *Vehicle Dynamics and Control* (Springer Verlag, 2005). His research interests include sensors and control systems for automotive and biomedical applications.

Dr. Rajamani has served as Chair of the IEEE Technical Committee on Automotive Control and on the editorial boards of the IEEE TRANSACTIONS ON CONTROL SYSTEMS TECHNOLOGY and the IEEE/ASME TRANSACTIONS ON MECHATRONICS. He was the recipient of the CAREER Award from the National Science Foundation, the 2001 Outstanding Paper award from the IEEE TRANSACTIONS ON CONTROL SYSTEMS TECHNOLOGY, the Ralph Teetor Award from the Society of Automotive Engineers, and the 2007 O. Hugo Schuck Award from the American Automatic Control Council.

Damrongrit Piyabongkarn received the B.E. degree from Chulalongkorn University, Bangkok, Thailand, the M.S. degree from the University of Texas, Arlington, and the Ph.D. degree from the University of Minnesota, Minneapolis, all in mechanical engineering.

He is currently a Senior Control Systems Specialist Engineer with the Innovation Center, Eaton Corporation, Eden Prairie, MN. His research interests include advanced controls, system identification, and state estimation, with applications to automotive systems, hybrid systems, electrohydraulic systems, and microsensor design.

Dr. Piyabongkarn received the 2007 O. Hugo Schuck Award, the Society of Automotive Engineers 2006 Arch Colwell Merit Award, and the 2003–2004 Doctoral Dissertation Fellowship from the University of Minnesota.

Vasilis Tsourapas received the M.S. degree in marine engineering from National Technical University of Athens, Athens, Greece, in 2003 and the M.S. degree in mechanical engineering and the Ph.D. degree in marine engineering from the University of Michigan, Ann Arbor, in 2005 and 2007, respectively. His Ph.D. research was funded by the Office of Naval Research, the National Science Foundation, and the Automotive Research Center, University of Michigan.

He is currently an Engineering Specialist with Innovation Center, Eaton Corporation, Eden Prairie, MN. His research interests include optimal controls, system optimization, and power management with applications to hybrid drivetrain optimization, vehicle dynamics, alternative power generation, and exhaust after-treatment systems.

Dr. Tsourapas received the Department of Defense Graduate Fellowship during 2005–2007.

Jae Y. Lew received the Ph.D. degree in mechanical engineering from Georgia Institute of Technology, Atlanta, in 1993.

He is currently with Innovation Center, Eaton Corporation, Eden Prairie, MN. Since his Ph.D. studies, he has gained 18 years of research and teaching experience in the fields of control, dynamics, robotics, and mechatronics. This comprises some five years as a Research Scientist with Pacific Northwest National Laboratory; six years as an Assistant/Associate (tenured) Professor with Ohio University, Athens; and seven years as a Chief Engineer with the Eaton Innovation Center. His research interests are in applying modern control theory to electromechanical and hydraulic systems, particularly active damping and contact control of large-structure systems, including construction equipment and offshore applications, wind power drivetrain control, vehicle stability control systems with active differentials, and powertrain control of electrical/hydraulic hybrid vehicles.

Dr. Lew is currently an Associate Editor for the IEEE TRANSACTIONS ON CONTROL SYSTEMS TECHNOLOGY. He received the ACC 2007 O. Hugo Schuck Award for the best application paper and the Society of Automotive Engineers 2006 Arch Colwell Merit Award.